IEEE Access
Multidisciplinary | Rapid Review | Open Access Journal

Received October 14, 2021, accepted October 27, 2021, date of publication October 29, 2021, date of current version November 8, 2021.

Digital Object Identifier 10.1109/ACCESS.2021.3124287

Hybrid Numerical Methodology for Efficient Design and Optimization of Transmit-Array Antennas, X-Band Application

JEANNE PAGES-MOUNIC[1,2], ALESSANDRO DE OLIVEIRA CABRAL JUNIOR[1,2], ANDRÉ BARKA[1], AND HAMZA KAOUACH[2]

[1]ONERA/DEMR, Université de Toulouse, 31055 Toulouse, France
[2]LAPLACE Laboratory, CNRS, Toulouse INP-ENSEEIHT, University of Toulouse, 31071 Toulouse, France

Corresponding author: André Barka (andre.barka@onera.fr)

This work was supported in part by the Region Occitanie under Research Project N◦ 2018 001223/ALDOCT-00384, and in part by the GENCI from which the full wave simulation results have been obtained using HPC resources under Grant c2014109083.

ABSTRACT This paper presents a complete hybrid numerical methodology for the efficient design and optimization of large-scale Transmit-Array (TA) antennas for modern telecommunication applications. There are four main components to the proposed work and methodology: 1) the implementation through Python scripts of a hybrid scheme based on the Friis analytical formula for linking gain and phase of the primary source and elementary cells of the studied transmit-array; 2) the implementation of a Particle Swarm Optimizer (PSO) for efficient characterization of the optimal phase distribution on the in-plane lens maximizing the gain of the antenna and minimizing the side-lobe levels for multiple fed TA antennas; 3) the implementation of a full-wave Finite element and Interconnecting domain decomposition (FETI) for the final analysis of the TA radiating performance; 4) the design, optimization, fabrication and proof of concept of an X band transmit-array including the focal source. This work presents the main functionalities of the hybrid Python/CST tool associated with phase compensation PSO, FETI implementation for transmit-arrays and as an application of this numerical strategy, a new compact unit-cell operating in the X-band (thickness of 3.2 mm) able to easily generate Phase Rotations (PR) necessary for TAs with phase compensation on the aperture. The proposed unit-cell is a completely symmetric design including a metallic via interconnecting two identical square patches (including a circular hole in the center and a microstrip line) by crossing through a ground plane. A particle swarm optimization (PSO) routine is proposed as a way to quickly optimize the phase distribution of the transmit-array unit-cells. The optimization routine is tested through multiple sources and focal ratios, demonstrating a reduction of over 50% of the volume occupied by the antenna, while keeping a high gain (19.5 dBi) and overall good performance.

INDEX TERMS Transmit-array, X-band, linear polarization, phase compensation, phase rotation, finite element methods, finite element tearing and interconnecting, FETI, domain decomposition methods, FACTOPO, CST microwave studio.

I. INTRODUCTION

Transmit-array (TA) is a popular cost-effective solution for high-gain antennas at millimeter wavelengths, particularly for telecommunications or space applications. A transmit-array consists in the illumination of radiating elements distributed over two arrays and fed by a focal source (Figure 1) as proposed for example in the X-band [1], [2]. To control the direction and the amplitude of the radiation pattern, intermediate circuits are placed between the two arrays and serve to modify the phase quantization of each unit-cell. They allow fast and accurate beamsteering of the main lobe and are therefore interesting solutions in the search for reconfigurable directional antennas [3], [4]. Recent work shows that TAs can also be a viable solution for Satcom on the Move ground terminals in the Ka-band [5], [6]. Recently, several configurations of transmit-arrays based on metasurfaces have been designed [7]–[10].

The associate editor coordinating the review of this manuscript and approving it for publication was Yilun Shang.

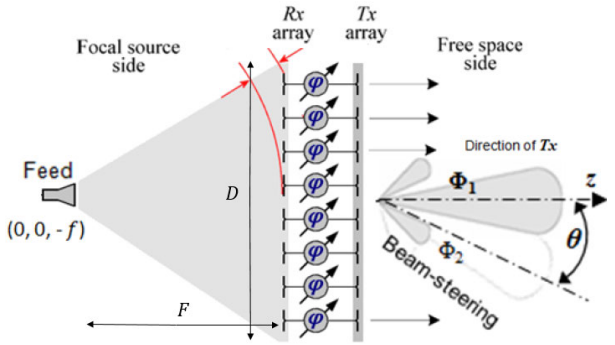

FIGURE 1. Transmit-array working principle (courtesy of [16]).

These research works have demonstrated that metasurfaces can be used to significantly reduce the size of TAs and to allow dual-band operation and multi-functions. As shown in Figure 1, the focal source is illuminating the TA with a spherical wave front and a plane wave front is created on the other side in the θ_0 direction.

The first contribution of the paper is a hybrid numerical methodology motivated by the fact that TAs are difficult to integrate in the final systems due to a focal ratio (F/D see Figure 1) that is normally in the range of 0.5 to 1 [1]. A high ratio is required for optimal performance, but drastically increases the volume occupied by the antenna. Recent realizations have been able to reduce this focal ratio in the Ka band by applying an intermediate flat plate polarizer lens antenna [5], which acts with a patch antenna to illuminate the TA with a virtual focus further away from the TA. The work done here was able to attain a focal ratio of 0.55, which is a good improvement but requires the use of a second lens between the patch source and the main lens, thus increasing costs and the complexity of the design. Other works have tried to counter this problem by employing multiple feeds closer to the TA, which act as one equivalent source with a longer virtual focus [11]. Though this work managed to effectively reduce the focal length by a factor of 50%, the use of four horn antennas as a feed would create difficulties in realizing a feeding network for them, as well as the non-negligible weight and volume of these antennas. This work also fails to detail how the phase distribution is optimized for the multiple feed case. The electromagnetic simulation of such large TA antennas is a challenging problem to be solved through Full Wave simulations, since the problem is not periodic and there are no symmetry planes to reduce the size of the problem. In addition, the small size of the unit-cells compared to the wavelength of the incident wave requires a highly detailed mesh for good accuracy. Although it is possible to obtain the antenna performance characteristics through commercially available software such as *ANSYS-HFSS* [12] and *CST Microwave Studio* [13], the memory resources and especially the time required for the simulation are highly prohibitive to the design phase of these antennas. For instance in [14], using FEKO's Method of Moments (MoM), a full wave simulation of a 30 × 30 reflect-array (analogous problem to a TA) in the Ka band takes about 27 hours of CPU time and 29.56 GB of memory. The work presented in this paper aims to propose a design and simulation methodology for large TA antennas that greatly reduces the full wave simulation efforts, which are however essential for the final analysis [15], thus reducing the time and memory consumption in the design phase of these antennas. Furthermore, this work also proposes the use of optimization techniques to achieve very low profiles for the final antenna, reducing the total occupied volume and allowing space constrained applications. A particle swarm optimization (PSO) routine is then proposed as a way to quickly optimize the phase distribution of the transmit-array unit-cells. For a multiple feed configuration, the simple algorithm allows the control of Side Lobe Levels (SLL) and axial gain.

The second contribution of the paper presents, as an application of the hybrid methodology, a novel X-band unit-cell architecture that improves the bandwidth while reducing the footprint. One particularity of the new unit-cell is that it transforms a vertical polarization into a horizontal polarization. It therefore behaves like a polarizer. The design offers a simple and good optimization of the impedance matching level based on its line theory model (introduced in the section V-A). Another particularity of this unit-cell is a lower profile (0.12 λ) compared to thick multi-layer structures such as Frequency Selective Surfaces (FSS). Compared to the state of the art, the new proposed unit-cell design (Figure 2) is perfectly symmetric [1] allowing i) reduction of the profile of the cell with a neglected mutual coupling between the adjacent cells and ii) easy phase shifting control [2] over a 360°-range by simply rotating the T-line (see Figure 2). It also enables the bandwidth to be increased by combining two coupling techniques between the Rx and Tx patch antennas, i.e. the coupling i) through the metallic via and directly ii) through the hole (slot) in the ground plane. One of the originalities of the proposed design is the internal feeding of the patch antenna compared to a standard patch excitation technique and the good mastery and comprehension of the impedance matching as explained in section V. The different impedances can be given by the EM simulation softwares (Z_{ant}, Z_{line} and Z_{via}). This unit-cell can be modelled as

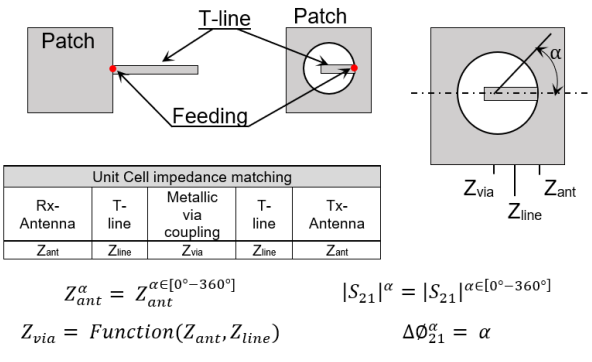

FIGURE 2. The proposed unit-cell; concept and model.

illustrated in Figure 2. The PSO optimization routine is tested through multiple sources and focal ratios, demonstrating a reduction of over 50% of the volume occupied by the antenna, while keeping a high gain ($\geq$ 19.5) dBi and overall good performance.

The first part of this paper will describe the hybrid analytical tool and the PSO optimizer for rapid design and optimization of TAs including the search for the optimal source. In the second part, we will discuss the FETI-2LM full-wave tool used for the analysis of the final design of the antenna. Next, we will describe in the third part the design of a new unit-cell operating in linear polarization and the simulated and measured performance of a 10λ × 10λ TA made up of 400 unit-cells populating the aperture through a 1-bit phase compensation and fed by an ATM 90-441-6(13971-D) horn source. Finally, the simulated performance of the TA fed by a microstrip patch array for demonstrating the reduction of over 50% of the volume occupied by the antenna will be described.

II. HYBRID ANALYTICAL/FULL-WAVE TOOL

In order to allow fast simulation of TA antennas, thus making parametric studies possible, a hybrid tool was developed to perform accurate simulations in under 0.5 seconds. This hybrid tool was proposed at first by [1] and developed as a *MATLAB* routine, and in our work is retrofitted with an object-oriented strategy coded in Python to efficiently design transmit-arrays and obtain their performance during parametric studies. The methodology used in this tool is based on the Friis formula for linking gain and phase of the primary source and the elementary cells characterized initially with full wave simulation tools.

In the simulations, the feed is considered to be well suited at the frequency of interest, so no mismatch is considered at this point. The power injected (and therefore radiated) by the feed is noted as P_1. Considering the free space propagation, the available power can be calculated at each of the cells using the Friis equation, Figure 3 summarizes the power budget. The phase center of the feed is considered to be at a point $(x_s, y_s, -f)$ and each cell has coordinates $(x_m, y_m, 0)$, thus the power link between these two objects can be calculated as:

$$P_3^m = \left(\frac{\lambda}{4\pi r_m}\right)^2 G_{SP}\left(\theta_{SP}^m, \varphi_{SP}^m\right) G_{AE}\left(\theta_{AE}^m, \varphi_{AE}^m\right) P_1 \quad (1)$$

where P_3^m is the available power on each of the m-unit cells, G_{SP} and G_{Rx} are, respectively, the source and unit cells Rx Gain, r_m the distance between the feed and the m-th cell and the couples $(\theta_{SP}^m, \phi_{SP}^m)$, $(\theta_{AE}^m, \phi_{AE}^m)$ are the incidence angles described in Figure 3. As the position of both feed and unit cells are known, the incidence angle at each lens can be calculated easily.

Each unit-cell of the TA is designed to provide a phase correction at a position (x, y) defined by:

$$\Phi_{lens}(x, y) = k_0\sqrt{x^2 + y^2 + f^2} - k_0 x \sin\theta_0 \quad (2)$$

where f is the focal distance. As a result and for the central position of the horn source, the phase at the output of the transmit-array is given by:

$$\phi_{out}(x, y) = -k_0 x sin\theta_0 \quad (3)$$

This leads to the conversion of the incoming spherical wave, into a planar phase front in the direction θ_0 in the plane $\phi = 0$.

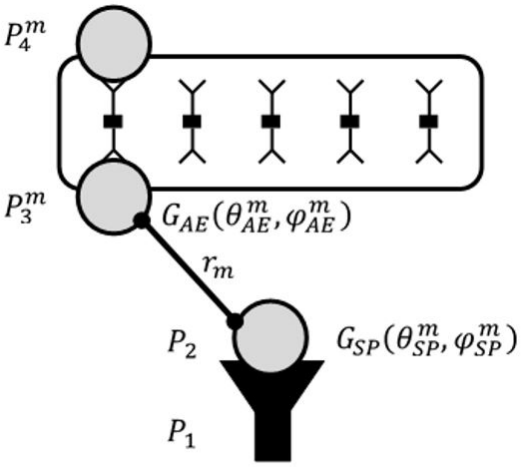

FIGURE 3. Parameters of the Friis formula.

To calculate the transmitted power to the Tx side, the unit cells will be modeled as the quadripole shown in Figure 4.

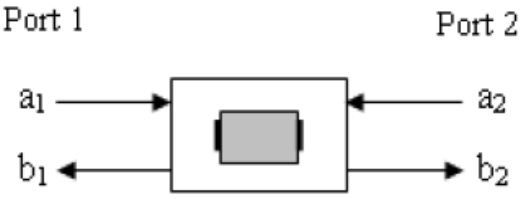

FIGURE 4. Quadripole model of unit cell.

As the incident power P_3^m is known through the Friis equation, the incident wave a_1^m can be easily calculated as:

$$a_1^m = \sqrt{P_3^m} e^{-j2\pi \frac{r_m}{\lambda}} e^{j\phi_{SP}^m} \quad (4)$$

where ϕ_{SP}^m is the phase of the incident field from the feed at the m-th cell. The total incident power is therefore calculated as:

$$P_3 = \sum |a_1^m|^2 \quad (5)$$

The computation of the transmitted waves is immediate through the use of the S matrix. Here, the incident wave a_2 is taken as zero, since the TA is treated in the transmission mode. Thus:

$$b_2^m = |S_{21}(\omega)| a_1^m e^{j\phi_{lens}^m} \quad (6)$$

where ϕ_{lens}^m is the transmission phase of the S_{21} parameter at the m-th cell, calculated through equation 2. By neglecting

the coupling between adjacent cells, the total power radiated by the Tx array is therefore:

$$P_4 = \sum |b_2^m|^2 \tag{7}$$

Since each transmitted wave is known, the total electric field radiated in the direction (θ, ϕ) can be obtained as the superposition of the fields radiated by each unit-cell at the Tx side. The array theory enables calculation of the power density of the total radiated field at an observation point (r, θ, ϕ) as:

$$|AF| = |\sum b_2^m e^{j2\frac{\pi}{\lambda}\sqrt{(x_m-x_s)^2+(y_m-y_s)^2}\sin\theta\cos(\phi-\phi_{AE}^m)}|^2 \tag{8}$$

$$S(\theta, \phi) = \frac{D_{lens}^{T_x}(\theta, \phi)}{4\pi r^2}.|AF(\theta, \phi)| \tag{9}$$

where $D_{lens}^{T_x}$ is the unit-cell directivity at the free space side (Tx side). The directivity of the TA can be obtained as the ratio of its power density and the total isotropic radiated power:

$$D(\theta, \phi) = \frac{S(\theta, \phi)}{S_i(\theta, \phi)} = \frac{4\pi r^2}{P_4} S(\theta, \phi) \tag{10}$$

The TA gain is calculated in a similar way, but instead of the total radiated power, the total input power is used:

$$G(\theta, \phi) = \frac{4\pi r^2}{P_1} S(\theta, \phi) = \frac{P_4}{P_1} D(\theta, \phi) = \eta_{41} D(\theta, \phi) \tag{11}$$

The hybrid tool makes it possible to carry out parametric studies very quickly by varying parameters such as the focal length and thus, to choose optimal values in the pre-dimensioning phases. Therefore, a parametric study can be performed to determine the optimal focal length, taking into account several performance indicators, in particular the axis gain (Figure 11), the Side Lobe Level (SLL), the power efficiency and the aperture efficiency as shown in Table 2 for several focal ratios F/D.

III. PSO OPTIMIZER

Considering for example the 20×20 transmit-array analyzed in section V, the optimization should find a 400 dimensional vector that satisfies the constraints of gain and SLL. This high dimensional problem would require a high computational effort to find the global minimum, which makes the use of gradient associated methods difficult due to the need for estimating a large gradient vector or an approximation to the Hessian matrix. Also, the search space of the multiple feed TA might not be differentiable, thus prohibiting the use of these methods.

A way around this high dimensional problem is to consider only solutions in which the phase gradient is symmetric around the x and y axis. In doing so, the 400 dimensional problem becomes a 100 dimensional one. Even though this method reduces the computational efforts to find a solution, the gradient associated methods still took too much time to converge (if ever). An optimization technique that has been used in solving many EM problems, such as phased array synthesis [17], [18], is the particle swarm optimization (PSO).

PSO is a stochastic population based optimization algorithm in which "particles", or candidate solution vectors, move around the optimization hyperspace to find the global maximum. A detailed explanation of the algorithm can be found in [19]. The principle of the algorithm is quite simple, given a starting point of a certain number of particles, the population of the "swarm", is initialized by randomly placing them around this initial guess. Each position is then scored by a cost function giving the "fitness" of these points. Each particle knows its personal best position (p_{best}) and the global best position ever passed by any of the particles (g_{best}). These values are updated after each iteration. To update the position of each particle, its velocity is defined as:

$$\begin{aligned} v_n &= \omega v_{n-1} + c_1 rand()(x_n - p_{best}) + c_2 rand()(x_n - g_{best}) \\ x_n &= x_{n-1} + v_n \end{aligned} \tag{12}$$

where ω, c_1, c_2 are coefficients controlling the impact of each term and *rand()* is a random number between 0 and 1. Equation 12 establishes that the each particle's velocity is composed of three components. ω is called the inertia weight which keeps the particle "traveling" in the same direction it was going at the last iteration. c_1 is the personal knowledge, it attracts the particle towards its best personal position. Finally, c_2 is the social knowledge weight that attracts the particle towards the global best found by the swarm. After a given number of iterations, the particles will have globally searched the optimization hyperspace and they may converge on a maximum point.

The simplicity of this method allows for easy adaptation of the routine, therefore making it capable of being applied to multiple transmit-array configurations with very little effort. Furthermore, it does not require differentiability (nor the approximation of derivatives) and it has the natural capacity to avoid local minima by its random movements. Inspired by other array synthesis problems [18], [20] and [17], an optimization module was developed. The goal was to maximize the axis gain, and keep the SLL under a determined threshold level SLL_{min}, thus the cost function was defined as:

$$f(x) = -Gain(\theta = 0^\circ) + \Pi(SLL) \tag{13}$$

$$\Pi(SLL) = \begin{cases} 0 & \text{if } SLL \leq SLL_{min} \\ \gamma |SLL - SLL_{min}| & \text{else} \end{cases} \tag{14}$$

where $\Pi(SLL)$ is a penalty function only applied if the SLL is over the threshold level, with the penalty able to be controlled through the γ parameter. Each particle corresponds to a 100 dimensional vector that is mapped as a phase distribution on the array. For each position of the optimization hyperspace, the hybrid tool is used to obtain the performance of the TA. Based on the cost function, each position is then scored and used to update the particles' velocities and position. To ensure better performance, the constriction factor proposed by [21] was applied, along with velocity clamping.

Upper and lower bounds for the positions were also used to ensure consistency with a 1-bit quantification.

A 50-particles population was considered, with a total of 10,000 iterations. The algorithm presented an overall good speed of execution, being able to execute a full iteration, that is 50 executions, in under 9 seconds. For the final results, a similar penalty regarding a minimum acceptable gain was also included in the cost function to avoid gain reduction. The gamma parameter impacts the overall evolution of the optimization in the sense that it may lead to a solution that privileges the constraint function over the gain optimization. The best compromise found was to set $\gamma_{SLL} = \gamma_{gain_{min}} = 3$.

Rather than starting the optimization of the phase distribution from a random initial point, the first approach is to divide the transmit-array into 4 ''independent'' parts. The phase distribution is calculated for a single source feeding each quadrant. The influence of the other feeds will, at first, be neglected and equation 2 is used. This new distribution (left image in Figure 5), presents a high gain, but a SLL that is too elevated. The 1-bit phase distribution on the array will be optimized to maintain the gain, while reducing the SLL.

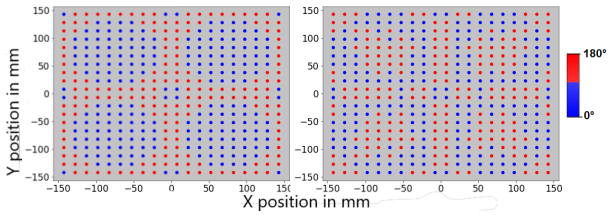

FIGURE 5. 1 bit phase gradient of the TA, initial guess (left) and final optimization result (right).

IV. FETI-2LM FINAL ANALYSIS

The final analysis of TA radiating performance can be performed with exact full wave methods. One of the most successful frequency domain computational methods for electromagnetic simulations [22] of antennas or microwave circuit engineering applications is the Finite Element Method (FEM). For computationally challenging TA applications especially, the FEM method requires the solution of problems with billions of unknowns. They are of course very difficult to solve with a single computational domain using commercial software such as CST Microwave Studio [13] or HFSS [12], especially when the problems of interest involve multi-scale geometries, with very small details compared to the wavelength. This is the case for X band or Ka-band transmit-array applications. The FETI-2LM method used to solve the Maxwell equations [23]–[25], splits the initial TA computational domain into non-overlapping sub-domains. The Finite Element solution of the local problems was first obtained with direct solvers [26] such as PARDISO. As proposed in a previous work [23], two Lagrange Multipliers are introduced to impose tangent field continuity at the interfaces of the sub-domains, and the reduced problem at the interfaces is solved with an iterative ORTHODIR method [27]. The realization of the complete meshing of the TA will require a considerable effort and would require considerable memory resources. This mesh is therefore not built into our simulation methodology.

Even with an automatic mesh splitter such as METIS [28], the TA being non-periodic, a single domain pre-treatment step would be long and difficult to implement. Our alternative strategy makes it possible to virtually build the mesh of the complete TA with only 3 types of sub-domain meshes (''lens unit cell'', ''empty unit-cell'' and ''horn'' described in Figure 6). As a consequence, our implementation of the FETI-2LM method only requires that the mesh has a reasonable size for each sub-domain. Each unit-cell at position (x, y) of the TA will be designed to provide a phase correction $\Phi_{lens}(x, y)$ (2). They comprise metallized layers of concentric square patches printed on substrate layers as described in Figure 6. For example, considering a 1-bit phase compensation application, the in-plane TA is designed with a set of $N_{elem} = 2$ elementary cells populating the TA.

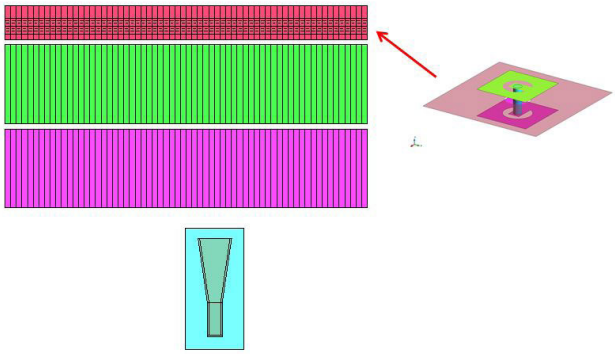

FIGURE 6. Exploded image of the TA domain decomposition (from bottom to top: horn (cyan), empty (purple and green), TA (red)).

In summary, the simulation strategy used is as follows:

- Step 1: Design and optimization of the $N_{elem} = 2$ unit-cell geometry with CST Microwave Studio [13]
- Step 2: Automatic mesh generation of the $N_{elem} = 2$ elementary unit-cells with the GID pre-processor [29]
- Step 3: Assignment of the $N_{elem} = 2$ elementary mesh cells populating the lens to the sub-domains and calculation cores
- Step 4: FETI-2LM simulations using massively parallel clusters
- Step 5: Extraction of the radiation patterns of the TA

V. APPLICATION TO THE DESIGN OF A LINEAR POLARIZATION TRANSMIT-ARRAY IN THE X BAND

For illustrating the efficiency of the hybrid numerical strategy proposed, we discuss the design and the optimization of a new low-profile X band unit-cell and the reduction of the volume occupied by the antenna (F/D) with a patch array as a focal source instead of an initial horn source.

A. PHASE ROTATION UNIT-CELL (DESIGN, MANUFACTURE AND MEASUREMENT)

The main idea of the new design consists in minimizing as much as possible the size of the unit-cell with the aim of increasing the number of cells populating a transmit-array and thus allowing its aperture efficiency to be increased. To achieve this, two patches and a metallic via have been placed in the center of the unit-cell (Figure 2. With this configuration, the patch antennas cannot be coupled because their impedances in the center are zero ($S_{11} = -1$). To modify these impedances, the antennas have been loaded by circular slot of radius R_{cyl} in the center of the unit-cell, and a microstrip line of width W_{line} (of impedance Z_{line}) has been used to connect the metallic via (of impedance Z_{via}) to the patch antenna (of impedance Z_{ant}). This new configuration (antenna with internal excitation) enables us introduction of a phase delay by rotating the transmission line (keeping the same Z_{ant}) and achievement of a perfect phase compensation (all the required phases on the array). The design challenge consists in matching the different impedances. The transmission line theory can be used (formula, lossless case):

$$Z_{via} = Z_{line}\frac{Z_{ant} + jtan(\frac{2\pi l}{\lambda_g})Z_{line}}{Z_{line} + jtan(\frac{2\pi l}{\lambda_g})Z_{ant}} \tag{15}$$

where $l = R_{cyl}$ and λ_g is the guided wavelength. A simple stub of length L_{step} was added as an additional design parameter for optimization, see Figure 7. The proposed unit-cell that is intended to be used for the manufacture of a 1-bit transmit-array is presented in Figure 7 and Table 1. It contains 3 metallic parts and operates at 10 GHz in linear polarization. The in-plane dimensions of the cell are 15 mm × 15 mm ($\lambda/2 \times \lambda/2$) and its thickness is 3.2 mm. The unit-cell is

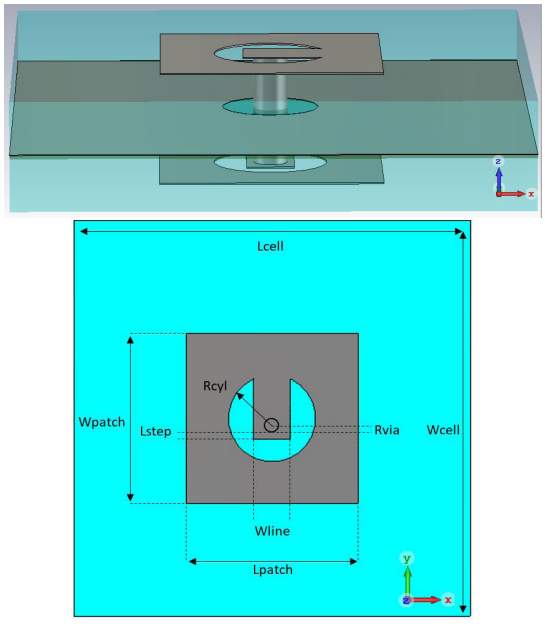

FIGURE 7. Unit-cell in sectional view.

TABLE 1. Unit-cell dimensions.

Lpatch	6.5 mm
Wpatch	6.45 mm
Rcyl	1.65 mm
Wline	1.4 mm
Rvia	0.5 mm
Lstep	0.3 mm
Lcell=Wcell	15 mm

made up of two patches connected by a metallic via. Between these two patches is inserted an 18 μm thick copper ground plane surrounded by 2 substrates (Rogers RO4003 1.524 mm thick with $\epsilon = 3.55$ relative permittivity and a dissipation factor tan δ of 0.0027). The two substrates are glued with a RO4450F pre-preg of thickness 100 μm. By rotating the upper patch, the unit-cell must allow Phase Rotations (PR) through phase-shifts on the transmission coefficient S21.

Based on these considerations, the design optimization of this unit-cell was carried out using the commercial electromagnetic CST simulation software [13]. Periodic array boundary conditions are imposed during these simulations permitting the mutual coupling between adjacent cells to be taken into account. The frequency response of the optimized cell is shown in Figure 8 (red curve) and is characterized by a bandwidth of nearly 900 MHz around 10 GHz which corresponds to a bandwidth of almost 9% and an insertion loss limited to −0.3 dB (green curve).

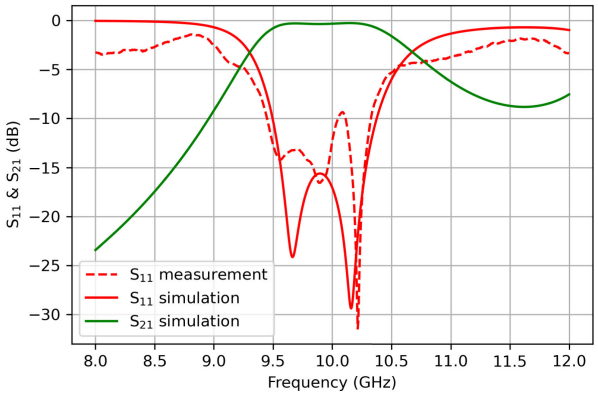

FIGURE 8. Simulated and measured unit-cell S-parameters.

The manufactured unit-cell measurements (Figure 9) were carried out using a WR-90 waveguide with suitable adaptor and a Wave Guide Measurement System (WGMS). The S11 measurements (Figure 8 dashed red curve) clearly show a −10 dB bandwidth of 870 MHz centered at 10 GHz which is reasonably similar to the simulated values.

Otherwise, the unit-cell has a simulated gain of 4.8 dBi which makes it a good candidate for transmit-array design. For this use, the cell is able to produce, by rotations of the upper patch, accurate phase-shifts on the lens transmit-array in-plane surface. As specified for example in [30], [31], the phase shift must be constant in frequency, in this case for

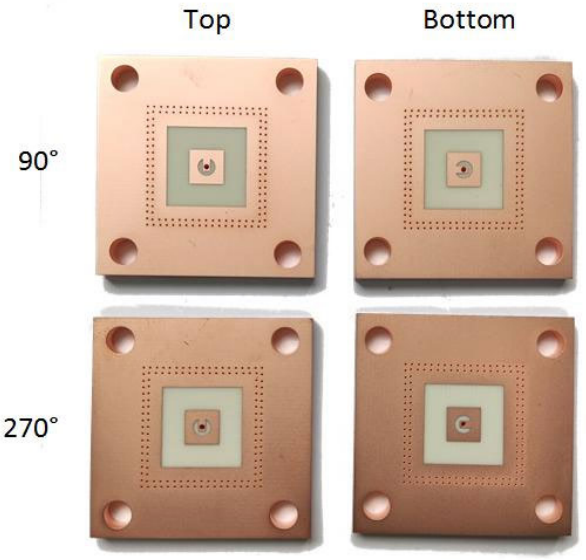

FIGURE 9. Top and bottom manufactured U slot patches: 90° (first row) and 270° (second row) unit-cells.

two rotations (90° and 270°), of 180° over the entire bandwidth. Our unit-cell permits rotation of the upper patch through +/− 90° allowing a 180° phase shift. Figure 9 and Figure 10 show the two cells thus designed and the validation by the simulation of the phase shift of 180° on the useful frequency band (90° in red and 270° in blue).

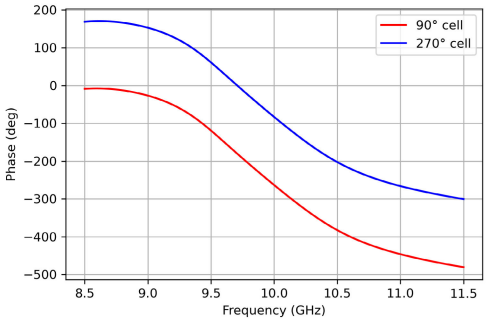

FIGURE 10. Phase-shift between the two cells.

B. INITIAL TRANSMIT-ARRAY IMPLEMENTATION WITH SINGLE FEED CONFIGURATION

A 20 × 20 transmit-array (TA) operating in the X-band and centered at 10 GHz is now considered. It consists of 400 unit-cells of dimensions 15 mm × 15 mm populated with the two unit-cells previously described in section V. The in-plane dimension of the array is then 300 mm × 300 mm and the primary source chosen is a rectangular 15 dB ATM 90-441-6(13971-D) horn operating between 8.2 GHz and 12.4 GHz.

The design of the TA is optimized in terms of focal length (F) with the hybrid analytical/exact tool presented in section II, to efficiently design transmit-arrays and obtain their performance.

As presented previously in section II, it is first necessary, using commercial software such as CST Microwave Studio [13], to obtain the gain and phase diagrams of the primary source (making it possible to determine the distribution of the electric field illuminating the array on the primary source side) as well as the unit-cell (allowing evaluation of the radiation performance of the transmit-array). The principle of a transmit-array is to associate with each unit-cell a phase gradient which then allows, once the array has been configured, a zenithal beam angle θ_0 to be obtained when the feed is at the central position (x = 0, y = 0). Each unit-cell of the TA has been designed to provide a phase correction $\Phi_{lens}(x, y)$ at position (x, y) and defined by equation (2). As a result and for the central position of the horn source, the phase at the output of the transmit-array is given by equation (3). However, the previous expression is a perfect compensation law and consequently there will be as many gradients as there are unit-cells, which greatly complicates the manufacturing. Thus, it is possible to consider a non-perfect phase quantization, with 2, 4 or 8 phase states. 1-bit phase compensation consists of two phase states: 90° and 270°, 2-bit compensation consists of four phase states, and so on. The greater the number of phase states, the greater the complexity of the array, the greater the precision of the phase gradient and therefore the precise angle θ_0 of beamforming. In our work, 1-bit phase compensation was chosen in order to simplify the design and manufacture of the transmit-array.

The hybrid tool makes it possible to carry out parametric studies very quickly by varying parameters such as the focal length and thus, select optimal values in the design. Thus, a parametric study was performed to determine the optimal focal length. For this, several parameters have been taken into account, in particular the axis gain (Figure 11), the Side Lobe Level (SLL), the power efficiency and the aperture efficiency as shown in Table 2 for several focal ratio F/D.

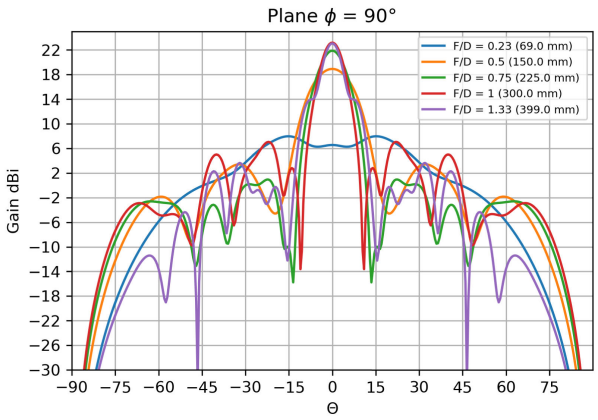

FIGURE 11. Gain as a function of F/D.

As a result of various parametric investigations carried out with the hybrid tool, the optimal focal ratio resulting in

TABLE 2. TA performance versus focal ratio F/D.

Focal Ratio	0.5	0.75	1.33
Gain max ($\theta = 0°$)	18.96	21.88	23.07
Directivity max ($\theta = 0°$)	20.69	23.63	25.41
SLL (dB)	-15.51	-20.93	-19.41
Power Efficiency (%)	66.56	66.76	58.3
Aperture Efficiency (%)	9.31	18.32	25.11

higher gains for this TA is 0.75 corresponding to a distance of 225 mm separating the source and the array. After studying the manufacturing complexity with several compensations (1-bit, 2-bit, 3-bit and perfect compensation), the model chosen for this TA is the 1-bit compensation (Figure 12), providing a gain difference of 3.4 dB compared to the perfect compensation and requiring only two different cells for populating the lens array. The maximum axial gain calculated by the hybrid tool for a 1-bit compensation model is 21.88 dBi. In order to confirm the efficiency of the TA before manufacture, full wave simulations are carried out with the Finite Element Tearing and Interconnecting (FETI) method in the frequency domain developed in [32] and briefly presented in section IV [15]. During the FETI simulation, the 20×20 physical array is completed by 2 empty elementary cells of the same size all around the array in order to remove the absorbing boundary surface far away from the physical array. The total number of sub-domains is then equal to 1153 (24×24 (lens array)+ 24×24 (empty array to adjust the focal distance) + 1 (horn)). Figure 13 shows the TA simulated setup and Figure 14 the simulated and measured gain patterns of the TA fed by the X-band horn in the H plane accessible with the measurement facility ($\phi = 90°$). Figure 16 shows the simulated E plane gain diagrams obtained with the Python hybrid tool and the FACTOPO full wave domain decomposition tool.

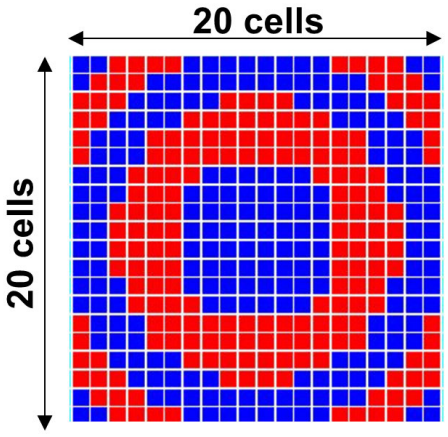

FIGURE 12. 1-bit compensation cells distribution of the 400 unit-cells TA prototype (PR = 90° in blue and PR = 270° in red).

During the FETI simulation, the domain decomposition solver takes into account the position of each cell on the array

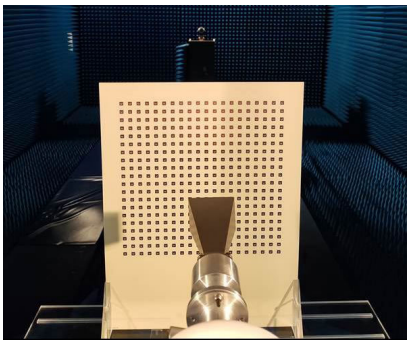

FIGURE 13. Measurements of the X-band TA prototype.

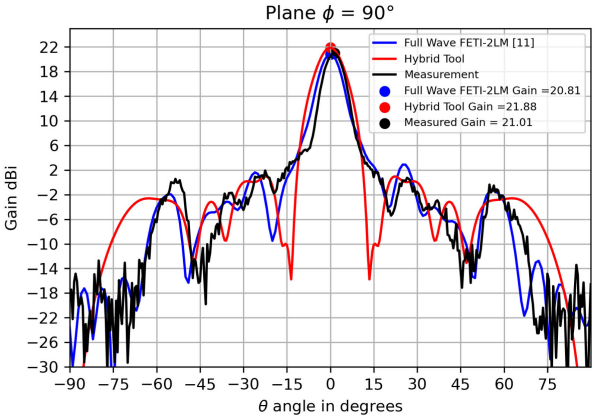

FIGURE 14. Measured and simulated gain pattern of the transmit-array for F/D = 0.75 (225 mm), H-plane ($\phi = 90°$).

and its orientation, given that we have considered a 1-bit compensation. Figure 12 shows the two types of cells considered, PR = 90° in blue and PR = 270° in red. Figure 14 shows that the full-wave axis gain (20.81 dBi on the red curve) is 1.07 dB less than the hybrid tool simulated gain (21.88 dBi on the red curve). This difference may be due to the fact that the hybrid-tool simulation does not take into account all electromagnetic phenomena such as diffractions by the edges of the array as well as the coupling effects between the source and the array. Both simulations are close to the measured gain pattern (21.01 dBi on the black curve) which is affected by a 1.5° shift, no doubt due to focal source misalignment. Additionally, both measurements and simulations showed a high cross-polarization (around 10 dBi) (Figure 15). Indeed, the large slot defined on the ground plane of the unit-cell design enables a non negligible amount of direct coupling between the incident wave and the upper patch. In Figure 17, showing the evolution of the simulated and measured axial gain as a function of the frequency, we observe that the gain is greater than 20 dBi in the frequency band [9.5 - 10.4 GHz] which is consistent with the 900 MHz bandwidth observed on the S_{11} measurements of the unit-cell (Figure 8). The experimental set-up allows for lens in-plane translation in front of the stationary primary feed. The evolution of the measured realized gain versus the beam tilt angle is presented

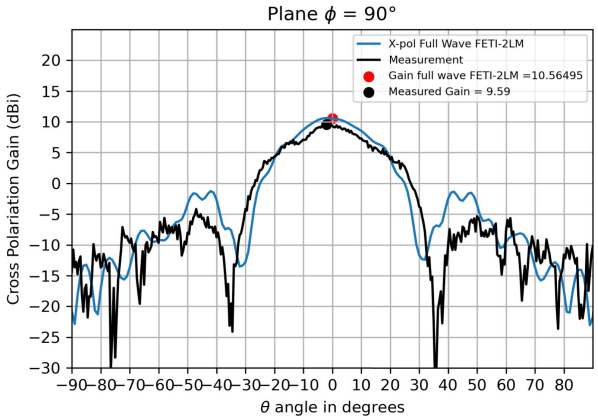

FIGURE 15. Measured and simulated (full-wave) cross polarization gains.

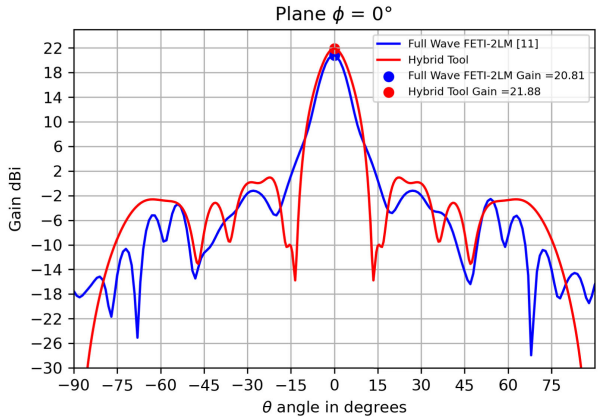

FIGURE 16. Full wave and hybrid simulated gain pattern of the transmit-array for F/D = 0.75 (225 mm), E-plane (ϕ = 0°).

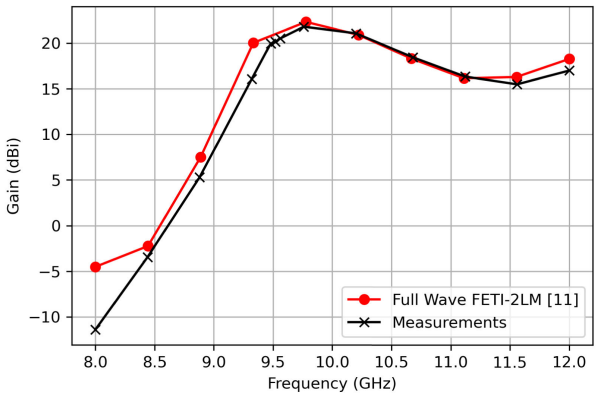

FIGURE 17. Measured and simulated (full-wave) gain versus frequency for F/D = 0.75 (225 mm).

in Figure 18. Measurements show that a beam scanning from −22.5° to +25° is achieved with 3 dB scan loss.

Table 3 shows the elapsed time of the different phases of the simulation methodology. The simulation time using CST, Hybrid tool and PSO routine are obtained on a standard PC with 1 Intel(R) Xeon(R) CPU E5-1603 @2.8GHz

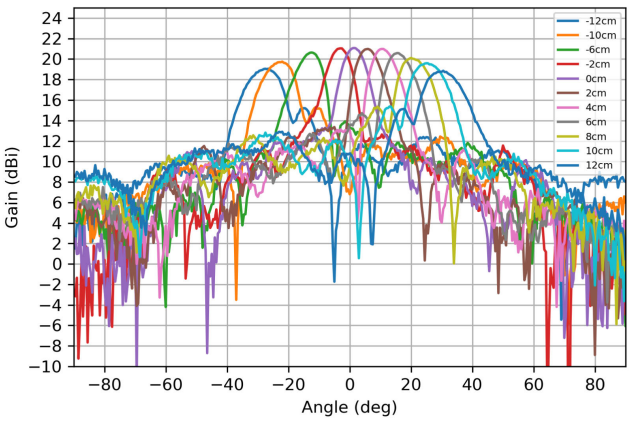

FIGURE 18. Measured gain patterns for beam tilt angles between −22.5° and 25°.

TABLE 3. Elapsed time consumed by each part of the hybrid numerical methodology.

Simulation	Elapsed Time
Feed Source (CST)	7 min 30 s
Unit-Cell (CST)	3 min 30s
Hybrid Code (Single Execution)	0.2 s
FACTOPO (per frequency)	53 min
PSO Routine (per iteration of 50 Particles)	9 s

processor. The FACTOPO simulation used 1153 Intel Xeon 2680v4 core processors. The simulation times demonstrate clearly the efficiency of the hybrid code for fast design of transmit-arrays.

C. TRANSMIT-ARRAY IMPLEMENTATION WITH MULTIPLE FEED CONFIGURATION

In order to achieve high gain with reduced focal ratios, a multiple feed TA is presented and designed with four sources placed at the center of each quadrant, as Figure 19 shows. The source separation is chosen to be $0.5D$, since it has been shown that the maximal gain for multiple feed TA is obtained around this value [33]. By approaching the four sources to the unit-cells, the illumination of the array becomes more uniform and thus higher directivities and gains can be obtained, since the four feeds will act as one equivalent source with a larger focal length. To avoid the use of bulkier sources like horn antennas, the optimization studies are carried out using standard microstrip patch antennas.

The objective of this work is not to achieve a large bandwidth and therefore the multiple feed source is designed to operate at 10 GHz following the steps described in [34] using the same substrate as that used for the unit-cell. Afterwards it is simulated using CST Microwave Studio and the results show a maximal gain of 6 dBi. To properly place the sources, a 2×2 array is designed using coaxial feeding and microstrip lines. The use of patches makes the feeding of the source much easier. A single 50 Ω coaxial cable is required to feed the structure and the power division is realized through power

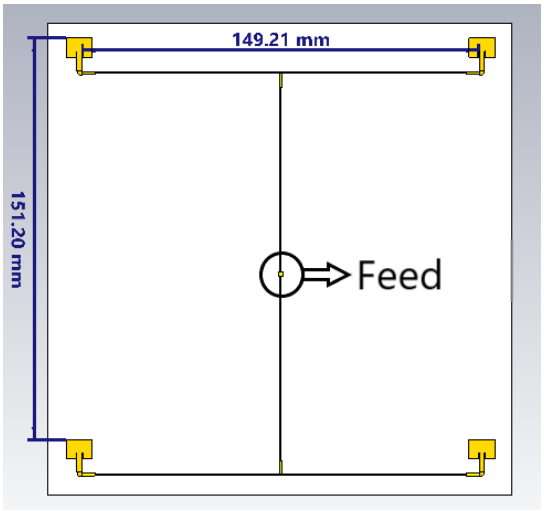

FIGURE 19. Square placement of the patch sources.

dividers with the microstrip lines, thus making the design simpler, cheaper and lighter.

The manufactured array reflection coefficient was measured and compared to simulations showing an overall good concordance and good matching at the central frequency, see Figure 20. The simulated losses on the microstrip lines were almost 1 dB due to their long length, causing a reduction of the TA gain and therefore taken into account in the hybrid simulation. The gain measurements closely matched the simulations, with a peak gain of 9 dBi as seen in Figure 21.

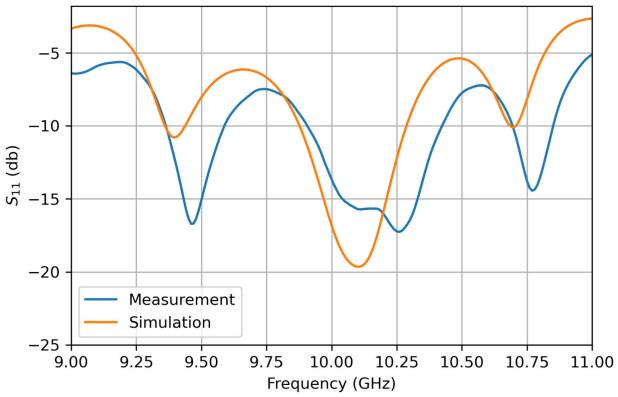

FIGURE 20. Reflection coefficient of manufactured patch array - Measurement and Simulation.

To analyse correctly the Figure 21, note that it presents the radiation pattern of four patch antennas taking into account the large distance between them (about 5 λ). So, it is not the radiation pattern of an array antenna composed by four elements.

It is worth mentioning that the simulations realized with the hybrid code include (in this case) 4 objects of the ''primary source'' or ''feed'' type. In other words, each source is treated as an independent antenna. Since the spacing between the elements is large ($5\lambda_0$), the inter-elements coupling is very

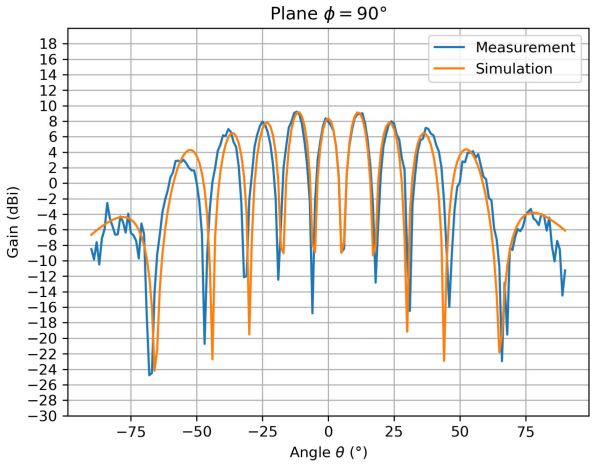

FIGURE 21. Realized gain of manufactured patch array - Measurement and Simulation at 10 GHz.

TABLE 4. Comparison of TA performances with a single or multiple feed.

		2×2 Patch Array	
Source	Single Patch	Initial Guess	Final Result
Directivity (dBi)	26.74	25.22	25.54
Gain (dBi)	19.49	19.2	19.55
SLL (dB)	-16.98	-8.72	-14.36
Aperture Efficiency (%)	37.5	26.42	28.44

reduced. In addition, for each patch, the TA lens is placed in the far field region, but regarding the whole patch array the lenses will not be in this region since its dimensions are much bigger than the ones from a single patch. Therefore, the use of the radiation pattern of the whole patch array will lead to false results from the hybrid code, justifying the modeling of the patch antennas as point sources.

In section V we designed an X-band 20 × 20 TA fed by a 16 dBi gain horn antenna with a focal ratio of 0.75. This optimization algorithm is used to achieve a reduction of at least 50% of the focal ratio by using multiple feeds. Figure 5 shows the comparison between the starting point of the optimization and the final solution for the proposed reduced ratio (0.375) found by the optimization routine. The radiation pattern of the multi-feed case is compared to that of a single patch (see Table 4) placed at a focal ratio of 0.75. As the 2 × 2 patch array acts as one single source placed further away from the TA lens, this ''single patch'' simulation gives the minimum achievable SLL for the same value of gain (19.5 dB). Finally, the multiple feed is also compared to the single horn feed TA presented earlier in Figure 22.

Table 4 shows that the optimization was able to achieve an SLL of - 14.31 dB, which represents an increase of only 2.67 dB when compared to the single patch feed. As shown, the optimization of the phase distribution enabled a reduced focal length without a major degradation of the radiation characteristics of the TA. In addition, the antenna efficiency increased, a high gain of 19.55 dBi was maintained and the total volume of the antenna was halved. This passage from

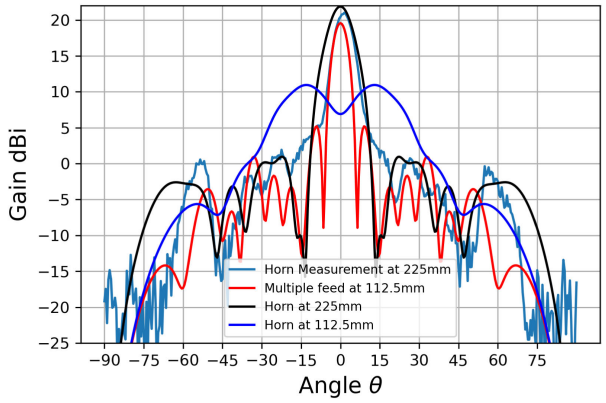

FIGURE 22. Radiation patterns of the multiple feed case compared to a single horn feed at multiple focal distances, $\phi = 90°$.

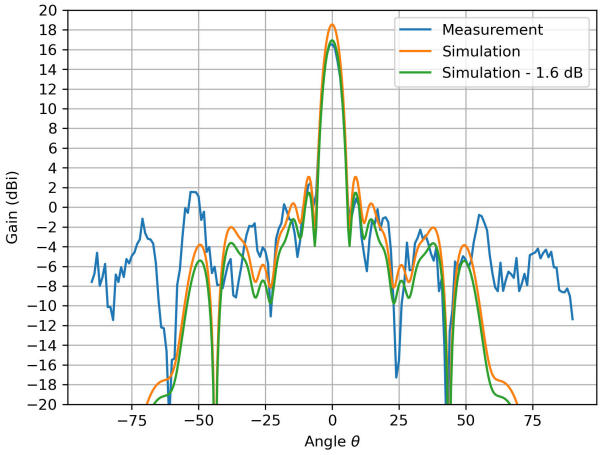

FIGURE 23. Measurement and Simulation of realized multiple feed TA, $\phi = 90°$.

a focal length of 225 mm to 112.5 mm allows for much easier integration in constrained spaces. Figure 26 shows the convergence of the PSO algorithm towards the optimal gain of the TA as a function of the number of cycles.

When compared to the single horn feed (see Figure 22), in the case of a large focal length (black and red curves), the multiple feed presents smaller gain, higher SLLs and smaller aperture efficiency. Nevertheless, in the case of a reduced focal ratio ($F = 112.5$ mm) it has much better performance than the horn (dark blue curve). In this case, the multiple feed presents a well-defined main beam and a higher axial gain, justifying its use as a solution for focal length reduction.

In Figure 23, we observe a good match of the simulated and measured radiation pattern of the multiple feed TA, with side lobes well placed. As the manufactured source presented 1 dB of loss in the transmission lines, this impact was considered for the final simulation which led to a simulated realized gain of 18.55 dBi. The gain measurements showed a difference of -1.6 dB when compared to the simulations. Multiple tests did not show evidence of misalignment between the antennas and this reduction was therefore attributed to edge effects on

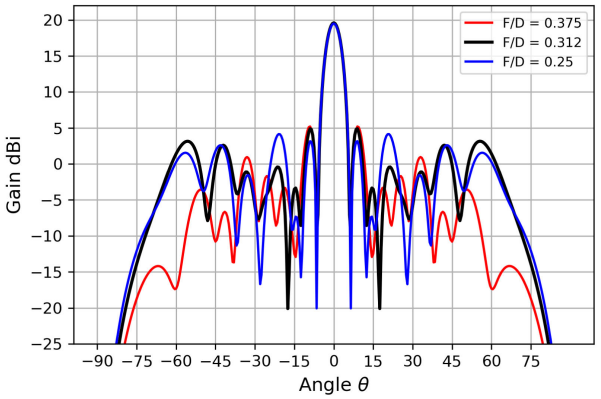

FIGURE 24. Radiation patterns of TA fed by a 2 × 2 microstrip patch array for different focal ratios, plane $\phi = 90°$.

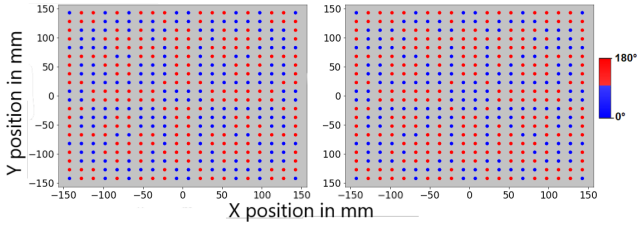

FIGURE 25. Optimized phase gradients of the TA for focal ratios of 0.312 (right) and 0.25 (left).

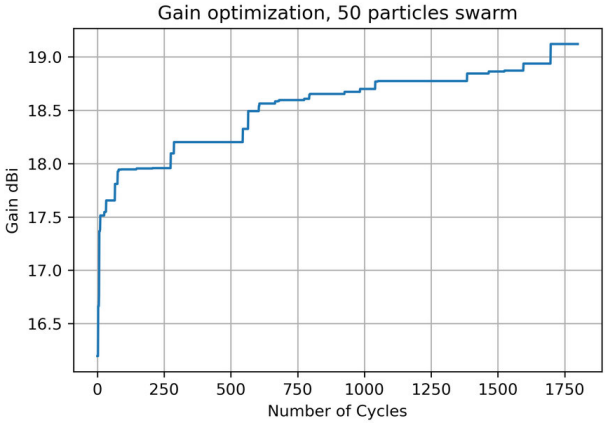

FIGURE 26. PSO Gain convergence.

the feeding patches, which could not be modeled in the hybrid code, and calibration problems with the anechoic chamber.

Since patch gains are low, the focal length reduction can be pushed further without loss of performance. Focal ratios of 0.312 and 0.25 were also studied, with both configurations having high gains and SLLs under the required threshold level of -14 dB as Figure 24 shows. The reduced focal ratio also reduces spillover losses and therefore increases the antenna power efficiency by up to 38%. The phase distributions showed in Figure 25 are remarkably close using the solution found for a ratio of 0.312 as a starting point for the 0.25 case, the optimization converged with less than 200 iterations.

VI. CONCLUSION

This paper presents a coherent hybrid numerical strategy for the design, optimization and final analysis simulations of TAs. As a demonstration of the numerical efficiency of the proposed methodology, the paper discusses the design, simulation and measurements of a new low profile and wide-band linearly polarized unit-cell. This cell shows interesting performance levels: a gain of 4.8 dBi, a simulated bandwidth of 870 MHz, a measured bandwidth of about 800 MHz and insertion losses of −0.3 dB. Following on from these results a 20 × 20 transmit-array has been designed with 1-bit phase compensation requiring 2 unit-cells, associated with a suitable horn primary source. The simulated performance of the TA is obtained with a very fast hybrid Python tool for the pre-design and a full-wave finite element domain decomposition method for the final analysis. For a focal ratio equal to 0.75, the full wave simulated gain is 20.81 dBi and the measured gain is 21.01 dBi, demonstrating that this transmit-array concept is very promising and theoretically well understood.

With the objective of reducing the overall volume of the antenna, a particle swarm optimization routine was tested through multiple simulations using different focal ratios and sources. The results show good performance, with gains above 19 dBi and side lobe levels under −14 dB. A volume reduction of more than 50% was achieved, allowing ratios as low as 0.25, with a gain reduction of only 2 dBi. The method is therefore an easy tool for the rapid design of space constrained transmit-array antennas, with performance that is easily adjustable through the cost functions. More advanced PSO techniques, such as cooperative swarms [19], will be investigated in future works to increase the algorithm performance.

REFERENCES

[1] H. Kaouach, L. Dussopt, J. Lanteri, T. Koleck, and R. Sauleau, "Wideband low-loss linear and circular polarization transmit-arrays in V-band," *IEEE Trans. Antennas Propag.*, vol. 59, no. 7, pp. 2513–2523, Jul. 2011.

[2] A. Clemente, L. Dussopt, R. Sauleau, P. Potier, and P. Pouliguen, "Wideband 400-element electronically reconfigurable transmitarray in X band," *IEEE Trans. Antennas Propag.*, vol. 61, no. 10, pp. 5017–5027, Oct. 2013.

[3] S. Ye, X. Liang, W. Wang, R. Jin, J. Geng, T. S. Bird, and Y. J. Guo, "High-gain planar antenna arrays for mobile satellite communications," *IEEE Antennas Propag. Mag.*, vol. 54, no. 6, pp. 256–268, Dec. 2012.

[4] J. R. Costa, C. A. Fernandes, G. Godi, R. Sauleau, L. Le Coq, and H. Legay, "Compact Ka-band lens antennas for LEO satellites," *IEEE Trans. Antennas Propag.*, vol. 56, no. 5, pp. 1251–1258, May 2008.

[5] E. B. Lima, S. A. Matos, J. R. Costa, C. A. Fernandes, and N. J. G. Fonseca, "Circular polarization wide-angle beam steering at Ka-band by in-plane translation of a plate lens antenna," *IEEE Trans. Antennas Propag.*, vol. 63, no. 12, pp. 5443–5455, Dec. 2015.

[6] S. A. Matos, E. Lima, J. S. Silva, J. R. Costa, C. A. Fernandes, N. J. G. Fonseca, and J. R. Mosig, "High gain dual-band beam-steering transmit array for satcom terminals at Ka-band," *IEEE Trans. Antennas Propag.*, vol. 65, no. 7, pp. 3528–3539, Jul. 2017.

[7] T.-J. Li, G.-M. Wang, T. Cai, H.-P. Li, J.-G. Liang, and J. Lou, "Broadband folded transmitarray antenna with ultralow-profile based on metasurfaces," *IEEE Trans. Antennas Propag.*, vol. 69, no. 10, pp. 7017–7022, Oct. 2021.

[8] H.-F. Huang and J. Zhang, "High-efficiency multifunction metasurface based on polarization sensitivity," *IEEE Antennas Wireless Propag. Lett.*, vol. 20, no. 8, pp. 1508–1512, Aug. 2021.

[9] M. Cai, Z. Yan, F. Fan, S. Yang, and X. Li, "Double-layer Ku/K dual-band orthogonally polarized high-efficiency transmitarray antenna," *IEEE Access*, vol. 9, pp. 89143–89149, 2021.

[10] L.-H. He, Y.-L. Ban, and G. Wu, "Dual-band quad-polarized transmitarray for 5G mm-wave application," *IEEE Access*, vol. 9, pp. 117520–117526, 2021.

[11] L. Di Palma, A. Clemente, L. Dussopt, R. Sauleau, P. Potier, andP. Pouliguen, "Reconfigurable transmit-array antenna with multiple focal sources," in *Proc. 8th Eur. Conf. Antennas Propag. (EuCAP)*, Apr. 2014, pp. 2308–2312.

[12] *Ansys HFSS*. [Online]. Available: https://www.ansys.com/products/electronics/ansys-hfss

[13] *CST Microwave Studio*. [Online]. Available: https://www.cst.com

[14] P. Nayeri, A. Z. Elsherbeni, and F. Yang, "Radiation analysis approaches for reflectarray antennas [antenna designer's notebook]," *IEEE Antennas Propag. Mag.*, vol. 55, no. 1, pp. 127–134, Feb. 2013.

[15] A. Barka, S. A. Matos, J. R. Costa, C. A. Fernandes, and H. Chreim, "Applying massively parallel computing to multiscale Ka dual-band transmit-array analysis using FETI-2LM," *IEEE J. Multiscale Multiphys. Comput. Techn.*, vol. 5, pp. 235–244, Jan. 2020.

[16] H. Kaouach, "Design and characterization of circularly polarized discrete lens antennas in 60-GHz band," *IEEE Antennas Wireless Propag. Lett.*, vol. 15, pp. 1200–1203, 2016.

[17] V. Zuniga, A. T. Erdogan, and T. Arslan, "Adaptive radiation pattern optimization for antenna arrays by phase perturbations using particle swarm optimization," in *Proc. NASA/ESA Conf. Adapt. Hardw. Syst.*, Jun. 2010, pp. 209–214.

[18] A. H. Abdelrahman, F. Yang, A. Z. Elsherbeni, P. Nayeri, and C. A. Balanis, *Analysis and Design of Transmitarray Antennas*. San Rafael, CA, USA: Morgan & Claypool, 2017, ch. 7, pp. 115–133.

[19] F. van den Bergh and A. P. Engelbrecht, "A cooperative approach to particle swarm optimization," *IEEE Trans. Evol. Comput.*, vol. 8, no. 3, pp. 225–239, Jun. 2004.

[20] D. W. Boeringer and D. H. Werner, "A comparison of particle swarm optimization and genetic algorithms for a phased array synthesis problem," in *IEEE Antennas Propag. Soc. Int. Symp. Dig. Held Conjunct With, USNC/CNC/URSI North Amer. Radio Sci. Meeting*, Jun. 2003, pp. 181–184.

[21] R. C. Eberhart and Y. Shi, "Comparing inertia weights and constriction factors in particle swarm optimization," in *Proc. IEEE Congr. Evol. Comput.*, vol. 1, Jul. 2002, pp. 84–88.

[22] J. Jin, *The Finite Element Method in Electromagnetics*, 2nd ed. New York, NY, USA: Wiley, 2002.

[23] F. Roux and A. Barka, *FETI Methods Chapter, Computational Electromagnetism—Recent Advances and Engineering Applications*, R. Mittra, Ed. New York, NY, USA: Springer, 2014.

[24] M. Vouvakis, Z. Zendes, and J. Lee, "A FEM domain decomposition method for photonic and electromagnetic band gap structures," *IEEE Trans. Antennas Propag.*, vol. 54, pp. 3000–3009, Feb. 2006.

[25] K. Zhao, V. Rawat, S.-C. Lee, and J.-F. Lee, "A domain decomposition method with nonconformal meshes for finite periodic and semi-periodic structures," *IEEE Trans. Antennas Propag.*, vol. 55, no. 9, pp. 2559–2570, Sep. 2007.

[26] (Oct. 2015). *Intel Mkl Pardiso*. [Online]. Available: https://software.intel.com/en-us/node/470282

[27] *Iterative Methods for Sparse Linear Systems*. Yousef Saad. Accessed: Jan. 2020. [Online]. Available: https://www-users.cs.umn.edu/~saad/books.html

[28] *Metis Serial Graph Partitioning and Fill Reducing Matrix Ordering*. Accessed: Jan. 2020. [Online]. Available: http://glaros.dtc.umn.edu/gkhome/views/metis

[29] *GID the Personal Pre and Post Processor*. Accessed: Jan. 2020. [Online]. Available: https://www.gidhome.com

[30] P. Naseri, S. A. Matos, J. R. Costa, C. A. Fernandes, and N. J. G. Fonseca, "Dual-band dual-linear-to-circular polarization converter in transmission mode application to *K*/*Ka*-band satellite communications," *IEEE Trans. Antennas Propag.*, vol. 66, no. 12, pp. 7128–7137, Dec. 2018.

[31] S. A. Matos, J. R. Costa, E. B. Lima, P. Naseri, C. A. Fernandes, and N. J. G. Fonseca, "Wide-angle mechanical scanning transmit-arrays for satellite Ka-band user terminals," in *Proc. IEEE Int. Symp. Antennas Propag. USNC/URSI Nat. Radio Sci. Meeting*, Jul. 2018, pp. 1445–1446.

[32] F.-X. Roux and A. Barka, "Block Krylov recycling algorithms for FETI-2LM applied to 3-D electromagnetic wave scattering and radiation," *IEEE Trans. Antennas Propag.*, vol. 65, no. 4, pp. 1886–1895, Apr. 2017.
[33] A. Clemente, L. Dussopt, R. Sauleau, P. Potier, and P. Pouliguen, "Focal distance reduction of transmit-array antennas using multiple feeds," *IEEE Antennas Wireless Propag. Lett.*, vol. 11, pp. 1311–1314, 2012.
[34] C. A. Balanis, *Antenna Theory: Analysis and Design*. Hoboken, NJ, USA: Wiley, 2005.

JEANNE PAGES-MOUNIC received the bachelor's degree in electronics, electrical energy and automation (EEA) from Jean-François Champollion University Center, Albi, in 2016, and the master's degree in electronics, embedded systems, and telecommunications (ESET) from Paul Sabatier University, Toulouse, in 2018. She is currently pursuing the Ph.D. degree in space antennas, particularly in transmit-arrays. Her thesis will be defended, at the end of 2021.

ALESSANDRO DE OLIVEIRA CABRAL JUNIOR started the bachelor's degree in electrical engineering at the Federal University of Pernambuco (UFPE), where he received a CAPES/BRAFITEC Grant for a double degree in France. He received the bachelor's and master's degrees in electronics and microwave engineering from the Toulouse-INP-École nationale supérieure d'électrotechnique, d'électronique, d'informatique, d'hydraulique et des télécommunications (ENSEEIHT), in 2021. He is currently engaged in a Ph.D. thesis at ONERA on research into active transmit-array antennas in the Ka-band.

ANDRÉ BARKA received the M.Sc. and Ph.D. degrees in applied mathematics from the University of Bordeaux, France, in 1986 and 1990, respectively, and the H.D.R. (Habilitation à Diriger des Recherches) degree from the University of Toulouse, in 2008. He joined ONERA, in 1989, where he is currently in charge of developing advanced multi-domain and multi-method techniques combining integral equations, finite element methods, and asymptotic techniques. From September 2016 to September 2017, he was a Guest Researcher with the Telecommunications Institute, University of Lisbon, Portugal, through a research convention with ONERA, the French DoD, and the University of Lisbon. He is also a Ph.D. Advisor of the GEET Doctoral School, Toulouse. He is a Senior Scientist with more than 20 years of research experience in computational electromagnetics, especially in domain decomposition methods, in various application fields, such as electromagnetic compatibility, radar cross section, and antennas. He was the Work-Package Manager for advanced modeling activities in the FP6 IPAS European Project and the H2020 EPICEA European/Canadian Project. His current research activities include the design and realization of new antenna concepts based on meta-materials as well as advanced domain decomposition methods, including finite element tearing and interconnecting (FETI) and integral equation domain decomposition methods (IE-DDM). He has been a Board Member of the *Computer Physics Communications* journal, since 2006, as a Computational Electromagnetic Specialist Editor.

HAMZA KAOUACH received the M.S. degree in high frequency communications systems from the University of Paris-Est Marne-la-Vallée, France, in 2006, and the Ph.D. degree in signal processing and telecommunications from the University of Rennes 1, France, in 2009. From 2006 to 2009, he was a Research Engineer at CEA-LETI, Grenoble, France. From 2010 to 2012, he was an Antenna and RF Engineer in industry at MATIS Group and PSA Peugeot Citroën Group, Paris, France. From July 2012 to August 2017, he was an Assistant Professor with the College of Engineering at Al-Lith (CEL), Department of Electronics and Communication Engineering (ECE), Umm Al-Qura University, Makkah, Saudi Arabia. Since September 2017, he has been an Assistant Professor with the Institut national polytechnique de Toulouse, University of Toulouse. His research interests include quasi-optic reconfigurable antennas, antenna arrays, and transmit-arrays at millimeter-wave frequencies.